



# An accurate one-dimensional theory for the dynamics of laminated composite curved beams



Gerardo Carpentieri<sup>a,\*</sup>, Francesco Tornabene<sup>b</sup>, Luigi Ascione<sup>a</sup>,  
Fernando Fraternali<sup>a</sup>

<sup>a</sup> Department of Civil Engineering, University of Salerno, Via Giovanni Paolo II 132, 84084 Fisciano, Italy

<sup>b</sup> DICAM Department, Alma Mater Studiorum, University of Bologna, Viale del Risorgimento 2, 40136 Bologna, Italy

## ARTICLE INFO

### Article history:

Received 30 May 2014

Received in revised form

24 September 2014

Accepted 30 September 2014

Handling Editor: S. Ilanko

Available online 24 October 2014

## ABSTRACT

We model the dynamic behavior of laminated curved beams on the assumption that the different layers of such structures are perfectly bonded at the interface and can show different flexural rotations from one another. We formulate a mechanical theory and a finite element model accounting for bending, shear, warping and extensional deformation modes, as well as radial, tangential and rotary inertias. The main novelty of the proposed theory consists of a generalization of layer-wise displacement approaches available in literature to the dynamics of beams with finite curvature. The work includes some numerical results related to the free vibration of laminated arches and showing different support conditions and aspect ratios to establish comparisons with different theories in the literature. We observe that an accurate mechanical modeling of curved laminated beams is crucial for correct estimation of the eigenfrequencies and eigenmodes of such structures within a 1D framework.

© 2014 Elsevier Ltd. All rights reserved.

## 1. Introduction

In recent years there has been a growth of scientific interest in composite materials in the civil engineering field because of the particular utility of composite laminated structures in technical applications. In fact, it is well known that these structures allow optimization of the mechanical response of the material as a function of the loading direction.

One-dimensional curved structures are particularly interesting because they are largely employed both as independent elements, such as curved bridges and roof structures, and as stiffening elements, such as thin curved plates [1–5]. Wood is a natural composite material largely employed in civil engineering, and has been recently rediscovered thanks both to the introduction of advanced manufacturing technologies (such as glued laminated timber or glulam), and progress in terms of fire resistance enhancement and cost reductions [6–8]. In many cases, wood is associated with other building materials like concrete, steel and glass [9–12]. The dynamic behavior of timber structures has recently been experimentally investigated through “table-shake” tests, showing that such structures exhibit rather good response to seismic excitations thanks to low weight and high flexibility [13–15].

\* Corresponding author.

E-mail addresses: [gcarpentieri@unisa.it](mailto:gcarpentieri@unisa.it) (G. Carpentieri), [francesco.tornabene@unibo.it](mailto:francesco.tornabene@unibo.it) (F. Tornabene), [l.ascione@unisa.it](mailto:l.ascione@unisa.it) (L. Ascione), [f.fraternali@unisa.it](mailto:f.fraternali@unisa.it) (F. Fraternali).

The dynamics of curved laminated beams is often studied through shell models requiring a considerably large number of degrees of freedom, unlike one-dimensional models. Available shell models are based upon first-order and higher-order shear deformation theories [16–18], equivalent single layer approaches, eventually including “zig-zag” displacement effects [16,19,20], layer-wise theories [20,21] (refer to the Carrera Unified Formulation [22,23], and the literature review in Mehdi and Mohamad [24]), and mesh-free approaches [25]. Different 1D models of laminated beams have been formulated by [1,5,26–33] over the last 25 years, mainly referring to straight elements.

The present work deals with an analytical and numerical study on the dynamics of curved laminated beams described through a layer-wise approach to the displacement field. The mechanical modeling of such structures is complicated by the inclusion of shear deformability [34], which is often accounted for by penalizing the first-order shear rigidity by means of a suitable shear coefficient [35–38]. In this paper, we assume that the single layers of a laminated curved beam can show different rotations from one another in respect of a perfect bonding constraint at the interface. The overall “zig-zag” displacement field of the laminate accounts for warping deformations of the cross-sections and an accurate description of the shear deformation.

The beam kinematics depends on  $n + 2$  generalized displacements, which consist of the flexural rotations of the  $n$  layers and the mean tangential and radial displacements of the laminate. The generalized constitutive laws derived assume orthotropic linearly elastic behavior at the material level. The overall mechanical model generalizes that proposed in Yuan and Miller [26] to beams with finite curvature of the centerline. The work includes a finite element approximation of the given beam model, which makes use of four-node, isoparametric elements of the Lagrange family. Some numerical results regarding the eigenmodes of vibration of laminated arches are presented and variously discussed in terms of different aspect ratios and boundary conditions. Comparisons are established with the simplified beam theory presented in Henrych [39], which neglects extensional and shear deformability, rotatory and tangential inertia effects, 2D shell models [19], and 3D finite element models based on 20-node brick elements, ABAQUS 6.12 [40]. The given results highlight that accurate kinematic modeling of curved laminated beams is relevant for correct estimation of the frequencies and modes of vibration of such structures.

## 2. Mechanical model

Let us consider the laminated curved beam illustrated in Figs. 1–3, on assuming that the beam axis may feature arbitrary curvature. We model the generic layer (or lamina) as a Timoshenko's beam (first-order shear deformation theory), and describe the corresponding displacement field through the following kinematic variables:

- $v_2^{(k)}(s^{(k)}, t)$  radial component of the displacement of the centerline  $\alpha^{(k)}$ ;
- $v_3^{(k)}(s^{(k)}, t)$  tangential component of the displacement of the centerline  $\alpha^{(k)}$ ;
- $\varphi^{(k)}(s^{(k)}, t)$  flexural rotation of the generic cross-section.

We also assume that adjacent layers are perfectly bonded at the interface, and characterize the overall kinematics of the laminated beam in terms of the flexural rotations of the  $n$  layers ( $\varphi^{(1)}, \varphi^{(2)}, \dots, \varphi^{(n)}$ ) and the following two displacement parameters:

$$\bar{v}_2 = v_2^{(1)} = v_2^{(2)} = \dots = v_2^{(n)} \tag{1a}$$

$$\bar{v}_3 = \frac{1}{h} \sum_{k=1}^n v_3^{(k)} h^{(k)} \tag{1b}$$

which respectively represent the mean radial and tangential displacements of the generic cross-section (Fig. 2).

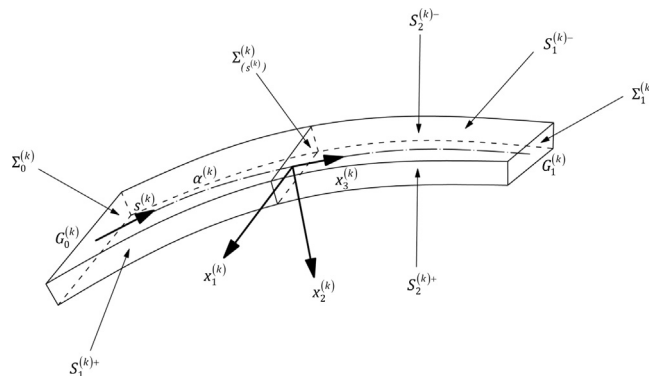


Fig. 1. Geometry of the  $k$ th layer.

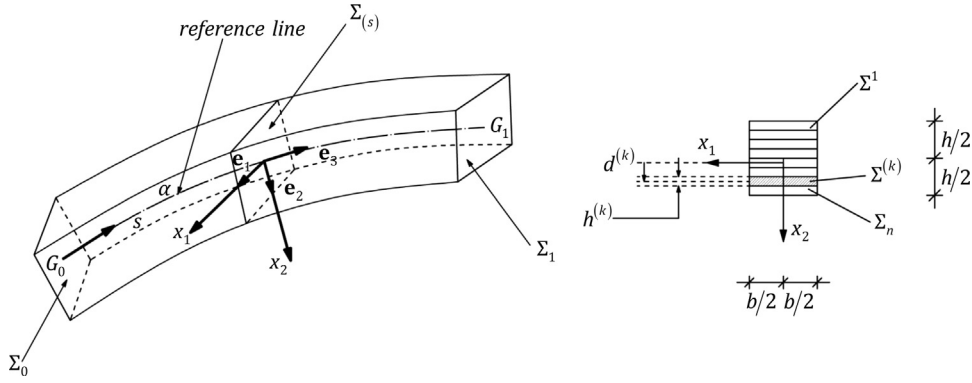


Fig. 2. Overall geometry of the laminated beam.

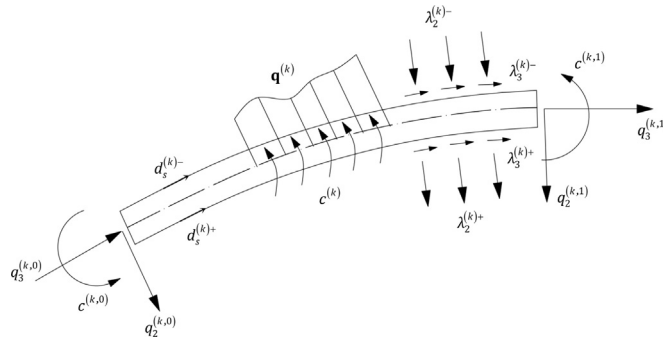


Fig. 3. Generalized forces acting on the kth layer.

The following matrix equation links the generalized displacements of the generic layer to the kinematic variables of the beam:

$$\mathbf{u}^{(k)} = \mathbf{A}^{(k)} \bar{\mathbf{u}} \quad \forall k = 1, 2, \dots, n \tag{2}$$

where

$$\mathbf{u}^{(k)} = [v_2^{(k)}, v_3^{(k)}, \varphi^{(k)}]^T \tag{3a}$$

$$\bar{\mathbf{u}} = [v_2, v_3, \varphi^{(k)}, \varphi^{(k)}, \dots, \varphi^{(k)}]^T \tag{3b}$$

$$A_{11}^{(k)} = 1, \quad A_{1i}^{(k)} = 0, \quad \forall i \neq 1 \tag{3c}$$

$$A_{21}^{(k)} = 0, \quad A_{22}^{(k)} = 1 \tag{3d}$$

$$A_{2,i+2}^{(k)} = h^{(i)} \left( h^{-1} d^{(i)} + \frac{1}{2} \text{sgn}(d^{(k)} - d^{(i)}) \right) \quad \forall i \in \{1, 2, \dots, n\} \tag{3e}$$

$$A_{3,k+2}^{(k)} = 1, \quad A_{3i}^{(k)} = 0, \quad \forall i \neq k+2 \tag{3f}$$

In the above equations,  $[\cdot]^T$  denotes the transpose of the array  $[\cdot]$ ; and  $\text{sgn}(x)$  denotes the signum function of the real number  $x$  ( $\text{sgn}(x) = +1, 0, -1$  when  $x > 0, x = 0, x < 0$ , respectively).

The equations of motion of the laminated beam can be enforced through the principle of virtual work, which leads us to the variational equation:

$$\int_{\alpha} \left( \sum_{k=1}^n \left( 1 - \frac{d^{(k)}}{\rho} \right) \boldsymbol{\sigma}^{(k)} \cdot \delta \boldsymbol{\epsilon}^{(k)} \right) ds = \int_{\alpha} \bar{\mathbf{q}} \cdot \delta \mathbf{u} \, ds - \int_{\alpha} \bar{\mathbf{M}} \ddot{\bar{\mathbf{u}}} \cdot \delta \bar{\mathbf{u}} \, ds + \bar{\mathbf{q}}_0 \cdot \delta \bar{\mathbf{u}}_0 + \bar{\mathbf{q}}_1 \cdot \delta \bar{\mathbf{u}}_1 \tag{4}$$

which holds for each virtual displacement  $\delta \bar{\mathbf{u}}$ , where  $(k \in [1, 2, \dots, n])$ ; refer to Fig. 3 for the notation):

$$\boldsymbol{\sigma}^{(k)} = [T^{(k)}, N^{(k)}, M^{(k)}]^T, \quad \boldsymbol{\epsilon}^{(k)} = [\gamma^{(k)}, \boldsymbol{\epsilon}^{(k)}, \chi^{(k)}]^T, \tag{5a}$$

$$\bar{\mathbf{q}} = \sum_{i=1}^n \left(1 - \rho^{-1} d^{(k)}\right) \mathbf{A}^{(k)T} \mathbf{q}^{(k)} + (1 + \rho^{-1} h/2) \mathbf{A}^{(1)T} \boldsymbol{\lambda}^{(1)-} + (1 - \rho^{-1} h/2) \mathbf{A}^{(n)T} \boldsymbol{\lambda}^{(n)+} \quad (5b)$$

$$\bar{\mathbf{M}} = \sum_{k=1}^n (1 - \rho^{-1} d^{(k)}) \mathbf{A}^{(k)} \mathbf{M}^{(k)} \mathbf{A}^{(k)} \quad (5c)$$

$$\bar{\mathbf{q}}_{\beta} = \sum_{k=1}^n \mathbf{A}^{(k)T} \mathbf{q}_{\beta}^{(k)} \quad (\beta = 0, 1) \quad (5d)$$

$$\mathbf{q}^{(k)} = [q_2^{(k)}, q_3^{(k)}, c^{(k)}]^T \quad (6a)$$

$$\boldsymbol{\lambda}^{(k)+} = [\lambda_2^{(k)-}, \lambda_3^{(k)+}, \lambda_3^{(k)+} h^{(k)}/2]^T \quad (6b)$$

$$\boldsymbol{\lambda}^{(k)-} = [\lambda_2^{(k)-}, \lambda_3^{(k)-}, -\lambda_3^{(k)-} h^{(k)}/2]^T \quad (6c)$$

$$\mathbf{q}_{\beta}^{(k)} = [q_2^{(k,\beta)}, q_3^{(k,\beta)}, c^{(k,\beta)}]^T \quad (\beta = 0, 1) \quad (6d)$$

$$\mathbf{M}^{(k)} = \begin{bmatrix} \mu^{(k)} A^{(k)} & 0 & 0 \\ 0 & \mu^{(k)} A^{(k)} & -\mu^{(k)} I^{(k)} / \rho^{(k)} \\ 0 & -\mu^{(k)} I^{(k)} / \rho^{(k)} & \mu^{(k)} I^{(k)} \end{bmatrix} \quad (6e)$$

In the above equations,  $\rho^{(k)}$  is the radius of curvature of the centerline  $\alpha^{(k)}$  of the  $k$ th layer which is related to the radius of curvature  $\rho$  of the centerline  $\alpha$  of the laminated beam through the equation:

$$\rho^{(k)} = \rho - d^{(k)} \quad (7)$$

$d^{(k)}$  denoting the radial abscissa of the centroid of the  $k$ th layer (Fig. 2).

The quantities  $T^{(k)}$ ,  $N^{(k)}$ ,  $M^{(k)}$  respectively denote the shear force, the axial force and the bending moment acting on the  $k$ th layer;  $\gamma^{(k)}$ ,  $\varepsilon^{(k)}$ ,  $\chi^{(k)}$  denote the generalized strains defined by

$$\gamma^{(k)} = \frac{dv_2^{(k)}}{ds^{(k)}} + \frac{v_3^{(k)}}{\rho^{(k)}} + \varphi^{(k)} = (1 - \rho^{-1} d^{(k)}) \left( \frac{dv_2^{(k)}}{ds} + \frac{v_3^{(k)}}{\rho} \right) + \varphi^{(k)} \quad (8a)$$

$$\varepsilon^{(k)} = \frac{dv_3^{(k)}}{ds^{(k)}} - \frac{v_2^{(k)}}{\rho^{(k)}} = (1 - \rho^{-1} d^{(k)}) \left( \frac{dv_3^{(k)}}{ds} - \frac{v_2^{(k)}}{\rho} \right) \quad (8b)$$

$$\chi^{(k)} = \frac{d\varphi^{(k)}}{ds^{(k)}} = (1 - \rho^{-1} d^{(k)}) \frac{d\varphi^{(k)}}{ds} \quad (8c)$$

The quantity  $\mu^{(k)}$  in Eq. (6e) denotes the mass density (per unit volume) of the  $k$ th layer; whereas  $A^{(k)}$  and  $I^{(k)}$  respectively denote the area and the moment of inertia of the cross-section of such a layer.

The constitutive laws relating to generalized stresses and strains are derived on the assumption that each layer is made up of a linearly elastic and orthotropic material with symmetry axes  $x_1^{(k)}$ ,  $x_2^{(k)}$ ,  $s^{(k)}$  (Fig. 1). The local orthotropic constitutive equations are written as follows:

$$\sigma_{33}^{(k)} = Q_{33}^{(k)} \varepsilon_{33}^{(k)} \quad (9a)$$

$$\sigma_{32}^{(k)} = 2Q_{44}^{(k)} \varepsilon_{32}^{(k)} \quad (9b)$$

where  $Q_{33}^{(k)}$  and  $Q_{44}^{(k)}$  denote the elasticity moduli of the material of the  $k$ th lamina, and the generalized constitutive laws are written in the following matrix form:

$$\boldsymbol{\sigma}^{(k)} = \mathbf{C}^{(k)} \boldsymbol{\varepsilon}^{(k)} \quad (10)$$

where

$$\mathbf{C}^{(k)} = \begin{bmatrix} A_{44}^{(k)} & 0 & 0 \\ 0 & A_{33}^{(k)} & B_{33}^{(k)} \\ 0 & B_{33}^{(k)} & D_{33}^{(k)} \end{bmatrix} \quad (11)$$

with

$$A_{44}^{(k)} = Q_{44}^{(k)} \left( A^{(k)} + \frac{J_p^{(k)}}{\rho^{(k)2}} \right) \tag{12a}$$

$$A_{33}^{(k)} = Q_{33}^{(k)} \left( A^{(k)} + \frac{J_p^{(k)}}{\rho^{(k)2}} \right) \tag{12b}$$

$$B_{33}^{(k)} = Q_{33}^{(k)} \left( \frac{J_p^{(k)}}{\rho^{(k)}} \right) \tag{12c}$$

$$D_{33}^{(k)} = Q_{33}^{(k)} J_p^{(k)} \tag{12d}$$

In Eq. (12), the quantity  $J_p^{(k)}$  denotes the “reduced” moment of inertia of the cross-section of the  $k$ th lamina, which is defined as follows:

$$J_p^{(k)} = \int_{\Sigma^{(k)}} x_2^{(k)2} \left( 1 - \frac{x_2^{(k)}}{\rho^{(k)}} \right) dx_1^{(k)} dx_2^{(k)} = \rho^{(k)2} \left( b \rho^{(k)} \ln \left( \frac{\rho^{(k)} + h^{(k)}/2}{\rho^{(k)} - h^{(k)}/2} \right) - b h^{(k)} \right) \tag{13}$$

### 3. Finite elements approximation

The dynamic problem (4) can be solved through a finite elements approach based on the subdivision of the centerline  $\alpha$  into  $N$  isoparametric elements with four nodes of the Lagrange family, Reddy [41] (Fig. 4). As regards the generic element “ $e$ ,” we write:

$$\bar{\mathbf{u}}(\xi, t) = \mathbf{F}(\xi) \bar{\mathbf{u}}^{(e)}(t) \tag{14a}$$

$$y(\xi) = \sum_{i=1}^4 \psi_i(\xi) y_i^{(e)}, \quad z(\xi) = \sum_{i=1}^4 \psi_i(\xi) z_i^{(e)}, \tag{14b}$$

where  $\bar{\mathbf{u}}^{(e)}$  is the following vector of the nodal displacements featuring  $4(n+2)$  entries:

$$\bar{\mathbf{u}}^{(e)} = [\bar{u}_1^{(e)}, \bar{u}_2^{(e)}, \bar{u}_3^{(e)}, \bar{u}_4^{(e)}]^T \tag{15a}$$

$$\bar{\mathbf{u}}_i^{(e)} = [v_2^{(i)}, v_3^{(i)}, \varphi^{(1,i)}, \dots, \varphi^{(n,i)}]^T \quad \forall i = 1, \dots, 4, \tag{15b}$$

$\mathbf{F}(\xi)$  is a  $(n+2) \times 4(n+2)$  matrix collecting the Lagrange cubic polynomials  $\psi_i(\xi)$ :

$$\mathbf{F}(\xi) = [\psi_1(\xi) \mathbf{I}^{(n+2)} | \psi_2(\xi) \mathbf{I}^{(n+2)} | \psi_3(\xi) \mathbf{I}^{(n+2)} | \psi_4(\xi) \mathbf{I}^{(n+2)}]; \tag{16}$$

$\mathbf{I}^{(n+2)}$  denotes the identity matrix of order  $n+2$ ; and  $y_i^{(e)}, z_i^{(e)}$  are the nodal coordinates referring to the Cartesian frame  $\{0, y, z\}$  shown in Fig. 4. The nodal displacements referring to such a frame are related to the “local” displacements  $\bar{\mathbf{u}}^{(e)}$  through the equation

$$\mathbf{U}^{(e)} = \mathbf{B}^e \bar{\mathbf{u}}^{(e)} \tag{17}$$

where  $\mathbf{B}^e$  denotes a suitable transformation matrix. Substituting Eq. (17) into Eq. (14a), we obtain the following expression of the displacement field of the generic element “ $e$ ”:

$$\bar{\mathbf{u}}(\xi, t) = \mathbf{F}(\xi) \mathbf{B}^{eT} \mathbf{U}^{(e)}(t) \tag{18}$$

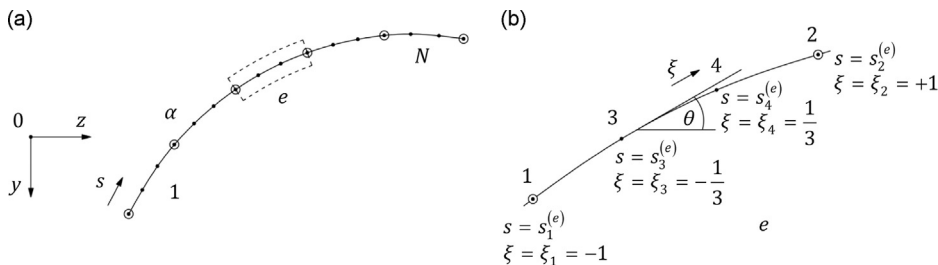


Fig. 4. Finite element discretization of the reference line  $\alpha$  (a) and schematic of the generic four-node element (b).

Making use of Eq. (18) and the following formula for the curvature of the reference line:

$$\rho(\xi)^{-1} = \left| \frac{dy}{d\xi} \frac{d^2z}{d\xi^2} - \frac{d^2y}{d\xi^2} \frac{dz}{d\xi} \right| \left[ \left( \frac{dy}{d\xi} \right)^2 + \left( \frac{dz}{d\xi} \right)^2 \right]^{-3/2} \tag{19}$$

we finally obtain the equations of motion of the finite element model in the standard form:

$$\mathbf{M}\ddot{\mathbf{U}} + \mathbf{K}\mathbf{U} = \mathbf{Q} \tag{20}$$

where  $\mathbf{U}$  and  $\mathbf{Q}$  are the vectors of nodal displacements and forces, respectively, featuring  $(n+2) \times (3N+1)$  entries (dofs);  $\mathbf{M}$  is the global mass matrix obtained through the assembly of the mass matrices  $\bar{\mathbf{M}}$  of the single elements (cf. Eqs. (5c) and (6)), and  $\mathbf{K}$  coincides with the linear term  $\mathbf{K}_0$  of the stiffness matrix given in Appendix B of [5].

#### 4. Numerical results

The present section makes use of the finite element model described in the previous section to carry out some numerical simulations of the free vibration modes and frequencies of laminated circular arches that show different aspect ratios and boundary conditions (Fig. 5). We analyze a circular arch clamped at both ends, and a circular arch clamped at one end and free at the other end. The examined arches are equipped with three layers composed of the same material.

We make use of a mesh of 10 four-node elements (for a total of 201 dofs), employing a Gauss formula with four points for the integration of the extensional and bending terms of the stiffness matrix, and a Gauss formula with three points for the integration of the shear terms of such a matrix. The analyzed examples consider two different arch geometries: a “slender arch” featuring the aspect ratios  $h/\rho=0.05$ ,  $b/\rho=0.025$ , and a “thick arch” showing  $h/\rho=0.4$ ,  $b/\rho=0.05$  (Fig. 5). We normalize the circular vibration frequencies  $\omega$  of the examined structures as follows:

$$\bar{\omega} = \left( \frac{\mu\rho^2}{Q_{33}} \right)^{1/2} \omega \tag{21}$$

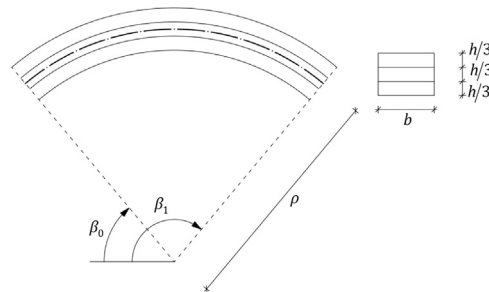


Fig. 5. Geometry of the circular arches analyzed in the numerical examples.

Table 1  
Normalized eigenfrequencies  $\bar{\omega}$  for the arch in Fig. 5 clamped at both ends.

| Slender arch: $h/\rho=0.05$ , $b/\rho=0.025$ |                |            |                        |
|--|----------------|------------|------------------------|
| Mode   | Present theory | 1D-Henrych | 2D-EDZ4                |
| 1  | 0.41330        | 0.44592    | 0.40650                |
| 2  | 0.67585        | 0.80993    | 0.66382                |
| 3  | 1.0424         | 1.4673     | 1.0322                 |
| 4  | 1.3616         | 2.1304     | 1.3082                 |
| 5  | 2.0596         | 3.1753     | 1.9272                 |
| Thick arch: $h/\rho=0.4$ , $b/\rho=0.05$     |                |            |                        |
| Mode   | Present theory | 2D-EDZ4    | 3D Abaqus <sup>®</sup> |
| 1  | 1.2169         | 1.1318     | 1.1315                 |
| 2  | 1.7272         | 1.4156     | 1.4131                 |
| 3  | 2.5319         | 2.3442     | 2.3439                 |
| 4  | 3.1999         | 3.4532     | 3.4443                 |
| 5  | 4.5427         | 4.4193     | 4.4079                 |

( $\beta_1 - \beta_0 = 80^\circ$ ,  $Q_{33}/Q_{44} = 2.5$ ).

The results obtained through the present theory are compared with those derived from the simplified beam theory presented in [39], which neglects extensional and shear deformations, rotary and tangential inertias, and supplementary numerical results deriving from 2D and 3D numerical schemes.

**Table 2**  
Normalized eigenfrequencies  $\bar{\omega}$  for the beam in Fig. 5 clamped at one end and free at the other.

| Slender arch: $h/\rho=0.05, b/\rho=0.025$ |                |            |                        |
|---|----------------|------------|------------------------|
| Mode                                      | Present theory | 1D-Henrych | 2D-EDZ4                |
| 1   | 0.02705        | 0.03759    | 0.02700                |
| 2   | 0.13560        | 0.15474    | 0.13501                |
| 3   | 0.41580        | 0.44615    | 0.41080                |
| 4   | 0.82908        | 0.88335    | 0.81193                |
| 5   | 1.3190         | 1.4673     | 1.2878                 |
| Thick arch: $h/\rho=0.4, b/\rho=0.05$     |                |            |                        |
| Mode                                      | Present theory | 2D-EDZ4    | 3D Abaqus <sup>®</sup> |
| 1   | 0.20194        | 0.19475    | 0.19472                |
| 2   | 0.75146        | 0.67333    | 0.67276                |
| 3   | 1.4035         | 1.3201     | 1.3199                 |
| 4   | 2.1465         | 1.8510     | 1.8494                 |
| 5   | 3.2999         | 2.6713     | 2.6676                 |

( $\beta_1 - \beta_0 = 80^\circ, Q_{33}/Q_{44} = 2.5$ ).

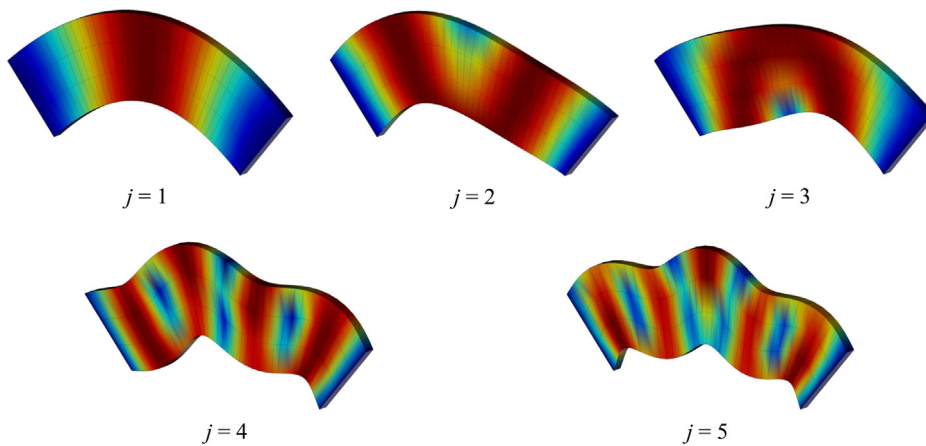


**Fig. 6.** First five vibration eigenmodes for the 2D-EDZ4 model of the thick arch clamped at both ends (the colored map refers to the norm of the current eigenvector). (For interpretation of the references to color in this figure legend, the reader is referred to the web version of this article.)

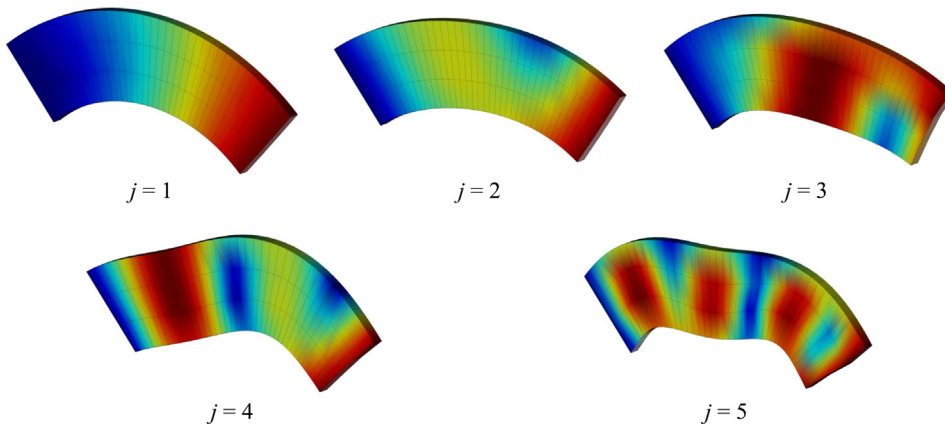


**Fig. 7.** First five vibration eigenmodes for the 2D-EDZ4 model of the thick arch clamped at one end and free at the other (the colored map refers to the norm of the current eigenvector). (For interpretation of the references to color in this figure legend, the reader is referred to the web version of this article.)

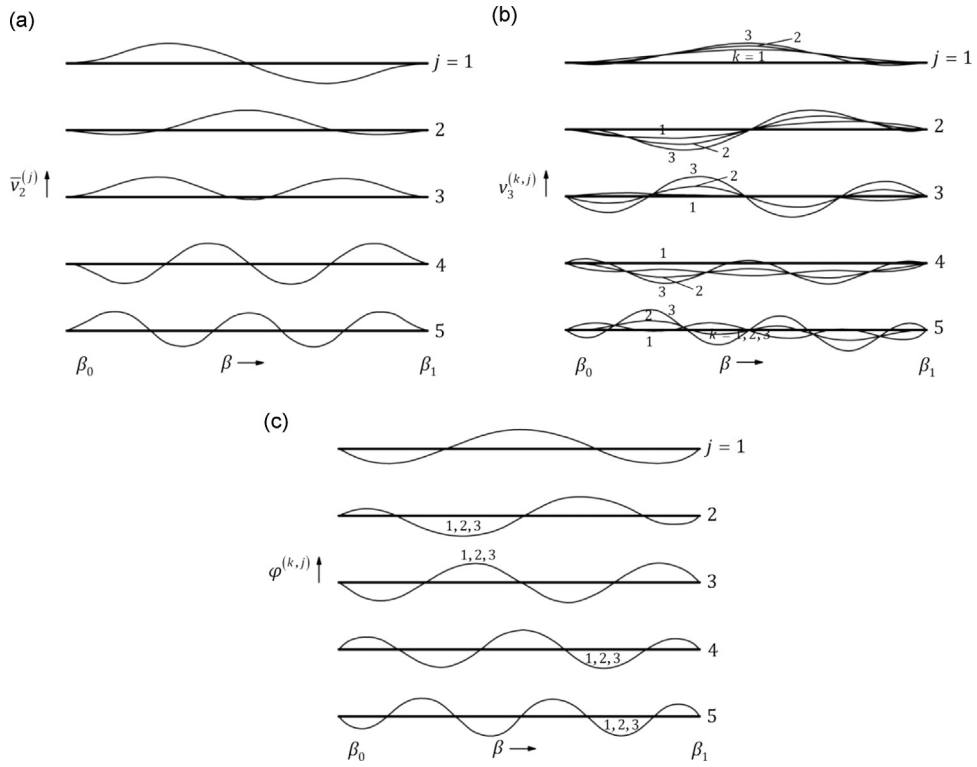


**Fig. 8.** First five eigenmodes corresponding to the present theory for the slender arch clamped at both ends: (a) mean radial displacement  $\bar{v}_2$ ; (b) mean tangential displacement  $\bar{v}_3$ ; and (c) flexural rotations  $\varphi^{(k)}$  of the different layers.

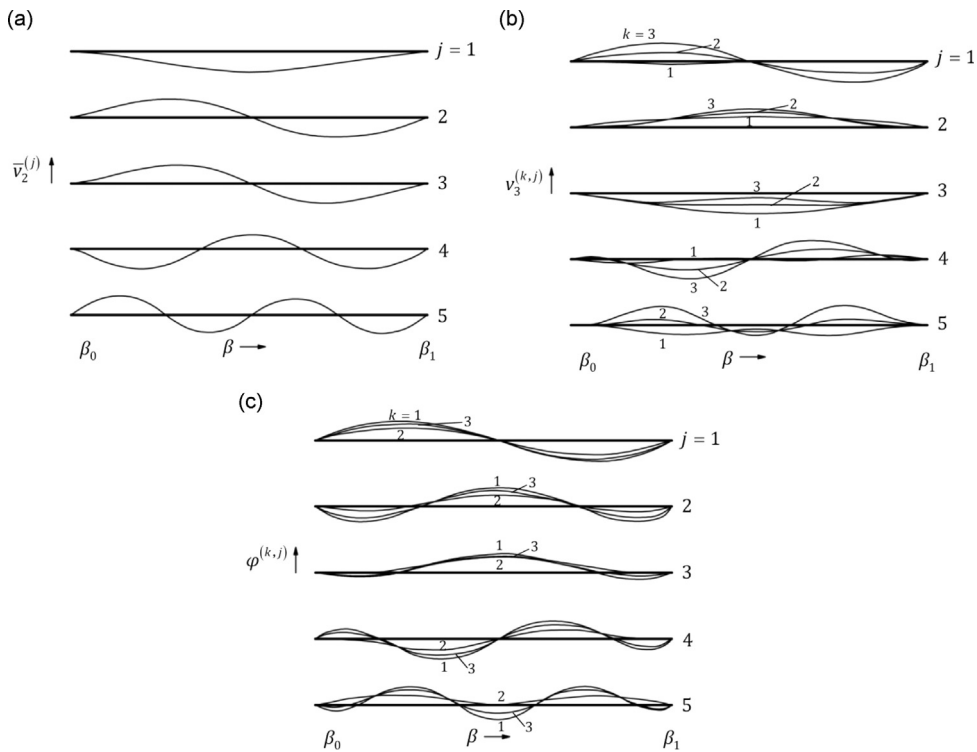


**Fig. 9.** First five eigenmodes corresponding to the present theory for the thick arch clamped at both ends: (a) mean radial displacement  $\bar{v}_2$ ; (b) mean tangential displacement  $\bar{v}_3$ ; and (c) flexural rotations  $\varphi^{(k)}$  of the different layers.

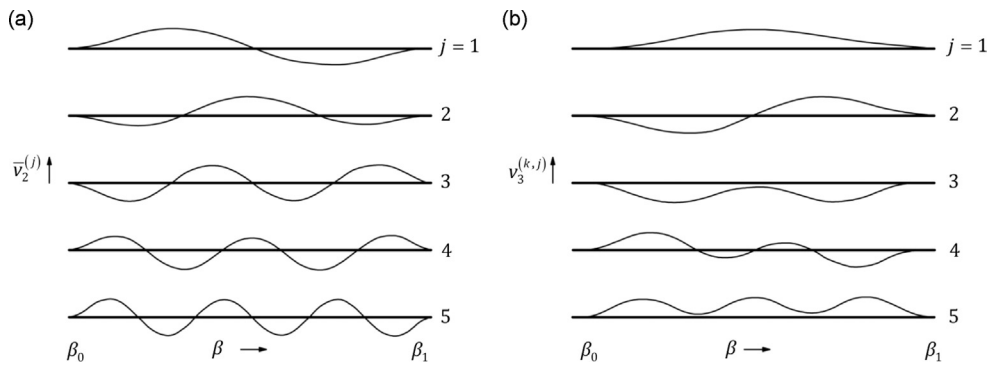


**Fig. 10.** First five eigenmodes corresponding to the theory of Henrych [39] for the slender arch clamped at both ends: (a) radial displacement of the centerline  $v_2$  and (b) tangential displacement of the centerline  $v_3$ .

The analyzed 2D model makes use of the equivalent single-layer theory EDZ4 theory presented by [19], which accounts for zig-zag effects (8370 dofs). The 3D comparative model is instead realized through ABAQUS 6.12 [40] and is composed of a brick element (C3D20) with 20 nodes for a total of 140,688 dofs.

Tables 1 and 2 show the normalized frequencies  $\bar{\omega}$  corresponding to the first five vibration modes of all the analyzed models, whereas Figs. 6–10 show the eigenmodes obtained through the 2D-EDZ4 model (Figs. 6 and 7), the present theory (Figs. 8 and 9), and the simplified theory by Henrych [39] (Fig. 10).

The results in Tables 1 and 2 highlight that the eigenfrequencies  $\bar{\omega}$  obtained through the present theory for the slender arch are in good agreement with those derived from the 2D-EDZ4 model, since the differences between the predictions of such theories range from 0.1% to 6%.

We note remarkable differences between the results of the above theories and those obtained from the simplified theory presented in Henrych [39], both in terms of eigenfrequencies (Tables 1 and 2), and in terms of eigenmodes (Figs. 8 and 10). We therefore conclude that the effects neglected in Henrych [39] (rotary and tangential inertias, extensional and shear deformations) already play an important role in the case of a slender beam.

Pausing to examine the thick arch examples, we observe a satisfactory match between the eigenfrequencies computed through the present theory and those deriving from the 2D-EDZ4 model, and the 3D Abaqus<sup>®</sup> model (Tables 1 and 2). We note that the eigenfrequencies obtained through the present theory exhibit differences ranging from 3% and 7% in correspondence with the first mode, and differences ranging between 6% and 19% for the other examined eigenmodes, as compared with the results of the above-mentioned 2D and 3D models. Such mismatches are explained by the 1D character of the present theory and the reduced number of dofs of the corresponding finite element model (201 dofs), which is remarkably lower than the number of dofs of the 2D EDZ4 model (8370 dofs) and the 3D Abaqus<sup>®</sup> model (140,688 dofs). The eigenmodes of the thick arch corresponding to the present theory (Fig. 9) are a good match with those predicted by the EDZ4 model (Fig. 6).

In the thick arch clamped at both ends, we notice a remarkable presence of warping effects, which are associated with different flexural rotations of the single layers along the beam axis (cf. Fig. 9c).

## 5. Conclusions

The numerical results presented in Section 4 allow us to conclude that a 1D, layer-wise model of the displacement of laminated curved beams is able to capture the main behaviors ruling the free vibrations of such structures, which include extension, shear, and warping deformation effects as well as transverse, rotary, and tangential inertias. We have generalized 1D layer-wise approaches available in literature [2,3,26] to the dynamics of laminated beams with arbitrary curvature of the longitudinal axis.

The above effects play a relevant role in eigenmodes and eigenfrequencies of laminated beams, and are also of fundamental importance in terms of interlaminar stresses and debonding criteria [1,3]. It has been shown that a simplified 1D theory accounting for pure bending response of curved laminated beams as presented by Henrych [39] does not accurately reproduce the above effects, either in the presence of slender geometries or in the case of thick beams. Overall, the beam theory presented in this work allows us to capture all such effects within a 1D framework, requiring a reduced number of degrees of freedom, as compared with more accurate 2D and 3D models.

## References

- [1] F. Fraternali, J.N. Reddy, A penalty model for the analysis of laminated composite shells, *International Journal of Solids and Structures* 30 (1993) 3337–3355, [http://dx.doi.org/10.1016/0020-7683\(93\)90088-0](http://dx.doi.org/10.1016/0020-7683(93)90088-0).
- [2] F. Fraternali, Energy release rates for delamination of composite beams, *Theoretical and Applied Fracture Mechanics* 25 (1996) 225–232, [http://dx.doi.org/10.1016/S0167-8442\(96\)00024-9](http://dx.doi.org/10.1016/S0167-8442(96)00024-9).

- [3] F. Fraternali, G. Bilotti, Non-linear elastic stress analysis in curved composite beams, *Computers & Structures* 62 (1997) 837–869, [http://dx.doi.org/10.1016/S0045-7949\(96\)00301-X](http://dx.doi.org/10.1016/S0045-7949(96)00301-X).
- [4] F. Fraternali, L. Feo, On a moderate rotation theory of thin-walled composite beams, *Composites Part B: Engineering* 31 (2000) 141–158, [http://dx.doi.org/10.1016/S1359-8368\(99\)00079-7](http://dx.doi.org/10.1016/S1359-8368(99)00079-7).
- [5] F. Fraternali, S. Spadea, L. Ascione, Buckling behavior of curved composite beams with different elastic response in tension and compression, *Computers & Structures* 100 (2013) 280–289, <http://dx.doi.org/10.1016/j.compstruct.2012.12.021>.
- [6] M. Piazza, R. Tomasi, R. Modena, *Strutture in Legno*, Hoepli, Milano, 2009.
- [7] J. König, Effective thermal actions and thermal properties of timber members in natural fires, *Fire and Materials* 30 (1) (2006) 51–63, <http://dx.doi.org/10.1002/fam.898>.
- [8] C. Maraveas, K. Miamis, E. Matthaios, Performance of timber connections exposed to fire: a review, *Fire Technology* (2013) 1–32, <http://dx.doi.org/10.1007/s10694-013-0369-y>.
- [9] D. Yeoh, M. Fragiaco, M. De Franceschi, K.H. Boon, State of the art on timber–concrete composite structures: literature review, *Journal of Structural Engineering* 137 (10) (2011) 1085–1095, [http://dx.doi.org/10.1061/\(ASCE\)ST.1943-541X.0000353](http://dx.doi.org/10.1061/(ASCE)ST.1943-541X.0000353).
- [10] M. Brunner, M. Romer, M. Schnüriger, Timber–concrete-composite with an adhesive connector (wet on wet process), *Materials and Structures* 40 (1) (2007) 119–126, <http://dx.doi.org/10.1617/s11527-006-9154-4>.
- [11] J.N. Rodrigues, A.M.P.G. Dias, P. Providência, Timber–concrete composite bridges: state-of-the-art review, *BioResources* 8 (4) (2013) 6630–6649.
- [12] O.B. Mekki, F. Toutlemonde, Experimental validation of a 10-m-span composite UHPFRC-carbon fibers–timber bridge concept, *Journal of Bridge Engineering* 16 (1) (2011) 148–157, [http://dx.doi.org/10.1061/\(ASCE\)BE.1943-5592.0000114](http://dx.doi.org/10.1061/(ASCE)BE.1943-5592.0000114).
- [13] J.W. Van de Lindt, S. Pei, S.E. Pryor, H. Shimizu, H. Isoda, Experimental seismic response of a full-scale six-story light-frame wood building, *Journal of Structural Engineering* 136 (10) (2010) 1262–1272, [http://dx.doi.org/10.1061/\(ASCE\)ST.1943-541X.0000222](http://dx.doi.org/10.1061/(ASCE)ST.1943-541X.0000222).
- [14] J.W. Van de Lindt, D.V. Rosowsky, W. Pang, S. Pei, Performance-based seismic design of midrise woodframe buildings, *Journal of Structural Engineering* 139 (8) (2013) 1294–1302, [http://dx.doi.org/10.1061/\(ASCE\)ST.1943-541X.0000653](http://dx.doi.org/10.1061/(ASCE)ST.1943-541X.0000653).
- [15] K. Luckasiri, T.H. Miller, R. Gupta, S. Pei, J.W. van de Lindt, A procedure for rapid visual screening for seismic safety of wood-frame dwellings with plan irregularity, *Engineering Structures* 36 (2012) 351–359, <http://dx.doi.org/10.1016/j.engstruct.2011.12.023>.
- [16] C.M. Wang, J.N. Reddy, K.H. Lee, *Shear Deformable Beams and Plates*, Elsevier, Singapore, 2000.
- [17] E. Carrera, Multilayered shell theories accounting for layerwise mixed description. Part 1: governing equations, *AIAA Journal* 37 (1999) 1107–1116, <http://dx.doi.org/10.2514/2.821>.
- [18] E. Carrera, Multilayered shell theories accounting for layerwise mixed description. Part 2: numerical evaluations, *AIAA Journal* 37 (1999) 1117–1124, <http://dx.doi.org/10.2514/2.822>.
- [19] F. Tornabene, E. Viola, N. Fantuzzi, General higher-order equivalent single layer theory for free vibrations of doubly-curved laminated composite shells and panels, *Composite Structures* 104 (2013) 94–117, <http://dx.doi.org/10.1016/j.compstruct.2013.04.009>.
- [20] E. Carrera, S. Brischetto, P. Nali, *Plates and Shells for Smart Structures: Classical and Advanced Theories for Modeling and Analysis*, Vol. 36, John Wiley & Sons, 2011.
- [21] J.N. Reddy, *Mechanics of Laminated Composite Plates and Shells*, CRC Press, College Station, 2003.
- [22] E. Carrera, Theories and finite elements for multilayered, anisotropic, composite plates and shells, *Archives of Computational Methods in Engineering* 9 (2) (2002) 87–140, <http://dx.doi.org/10.1007/BF02736649>.
- [23] E. Carrera, Theories and finite elements for multilayered plates and shells: a unified compact formulation with numerical assessment and benchmarking, *Archives of Computational Methods in Engineering* 10 (3) (2003) 215–296, <http://dx.doi.org/10.1007/BF02736224>.
- [24] H. Mehdi, S.Q. Mohamad, Vibrations of straight and curved composite beams: a review, *Composite Structures* 100 (2013) 218–232, <http://dx.doi.org/10.1016/j.compstruct.2013.01.001>.
- [25] F. Fraternali, C.D. Lorenz, G. Marcelli, On the estimation of the curvatures and bending rigidity of membrane networks via a local maximum-entropy approach, *Journal of Computational Physics* 231 (2012) 528–540, <http://dx.doi.org/10.1016/j.jcp.2011.09.017>.
- [26] F.G. Yuan, R.E. Miller, A new finite element for laminated composite beams, *Composite Structures* 31 (1989) 737–745, [http://dx.doi.org/10.1016/0045-7949\(89\)90207-1](http://dx.doi.org/10.1016/0045-7949(89)90207-1).
- [27] A.G. Razaqpur, H. Li, Refined analysis of curved thin-walled multicell box-girder, *Composite Structures* 53 (1) (1994) 131–142, [http://dx.doi.org/10.1016/0045-7949\(94\)90136-8](http://dx.doi.org/10.1016/0045-7949(94)90136-8).
- [28] J.M. Segura, G. Armengaud, Analytical formulation of stresses in curved composite beams, *Archive of Applied Mechanics* 68 (3–4) (1998) 206–213, <http://dx.doi.org/10.1007/s004190050158>.
- [29] R.K. Kapania, J. Li, A formulation and implementation of geometrically exact curved beam elements incorporating finite strains and finite rotations, *Computational Mechanics* 30 (5–6) (2003) 444–459, <http://dx.doi.org/10.1007/s00466-003-0422-7>.
- [30] C. Chang, D.H. Hodges, Stability studies for curved beams, *Journal of Mechanics of Materials and Structures* 4 (7–8) (2009) 1257–1270.
- [31] I. Ecsedi, K. Dluhi, A linear model for the static and dynamic analysis of nonhomogeneous curved beams, *Applied Mathematical Modelling* 29 (12) (2005) 1211–1231, <http://dx.doi.org/10.1016/j.apm.2005.03.006>.
- [32] H.J. Dagher, D.J. Bannon, W.G. Davids, R.A. Lopez-Anido, E. Nagy, K. Goslin, Bending behavior of concrete-filled tubular FRP arches for bridge structures, *Construction and Building Materials* 37 (2012) 432–439, <http://dx.doi.org/10.1016/j.conbuildmat.2012.07.067>.
- [33] W. Jung, J. Park, S. Kim, A study on the behavior characteristics of curved FRP concrete composite panel, *Advanced Materials Research* (2012) 375–380, <http://dx.doi.org/10.4028/www.scientific.net/AMR.557-559.375>.
- [34] A. Bhimaraddi, A.J. Car, P.J. Moss, Generalized finite element analysis of laminated curved beams with constant curvature, *Computers & Structures* 31 (1989) 309–317, [http://dx.doi.org/10.1016/0045-7949\(89\)90378-7](http://dx.doi.org/10.1016/0045-7949(89)90378-7).
- [35] R.D. Mindlin, H. Deresiewicz, Timoshenko's shear coefficient for flexural vibrations of beams, Technical Report No. 10, ONR Project NR064-388, Department of Civil Engineering, Columbia University, New York, 1953.
- [36] L.E. Goodman, J.G. Sutherland, Discussion of paper: Anderson, R.A., Flexural vibrations in uniform beams according to Timoshenko theory, *Journal of Applied Mechanics* 21 (1954) 202–204.
- [37] G.R. Cowper, The shear coefficient in Timoshenko's beam, *Journal of Applied Mechanics* 33 (1966) 335–340, <http://dx.doi.org/10.1115/1.3625046>.
- [38] J.M. Whitney, Shear correction factor for orthotropic laminates under static loads, *Journal of Applied Mechanics* 40 (1973) 302–304, <http://dx.doi.org/10.1115/1.3422950>.
- [39] J. Henrych, *The Dynamics of Arches and Frames*, Elsevier Publishing Company, Madison, 1981.
- [40] ABAQUS 6.12, Online documentation, Dassault Systèmes Simulia Corp., Providence, 2012.
- [41] J.N. Reddy, *An introduction to the Finite Element Method*, McGraw-Hill, New York, 1984.